



A novel network-based controller design for a class of stochastic nonlinear systems with multiple faults and full state constraints

Na Li, Yu-Qun Han, Wen-Jing He & Shan-Liang Zhu

To cite this article: Na Li, Yu-Qun Han, Wen-Jing He & Shan-Liang Zhu (2024) A novel network-based controller design for a class of stochastic nonlinear systems with multiple faults and full state constraints, *International Journal of Control*, 97:4, 651-661, DOI: [10.1080/00207179.2022.2163297](https://doi.org/10.1080/00207179.2022.2163297)

To link to this article: <https://doi.org/10.1080/00207179.2022.2163297>



Published online: 03 Jan 2023.



Submit your article to this journal [↗](#)



Article views: 259



View related articles [↗](#)



View Crossmark data [↗](#)



Citing articles: 11 View citing articles [↗](#)



A novel network-based controller design for a class of stochastic nonlinear systems with multiple faults and full state constraints

Na Li , Yu-Qun Han , Wen-Jing He  and Shan-Liang Zhu 

School of Mathematics and Physics, Qingdao University of Science and Technology, Qingdao, People's Republic of China

ABSTRACT

In this paper, the control issue of adaptive fault-tolerant is studied for a class of stochastic nonlinear systems with multiple faults and full state constraints, with multiple faults including the actuator faults and the external system fault. The problem with full state constraints are solved by constructing a logarithmic barrier Lyapunov functions (BLFs). By integrating multi-dimensional Taylor network (MTN) technology into the backstepping process, a new adaptive MTN-based fault-tolerant controller is designed. On the basis of considering multiple faults, the proposed control strategy can ensure that all signals in the closed-loop system are semi-global ultimately uniformly bounded (SGUUB) in probability, and all states of the system are constrained within the given boundary. Finally, three simulation examples are given to illustrate the effectiveness and practicability of the proposed control strategy.

ARTICLE HISTORY

Received 25 April 2022
Accepted 21 December 2022

KEYWORDS

Stochastic nonlinear systems;
full state constraints;
multiple faults;
multi-dimensional Taylor
networks

1. Introduction

With the development of nonlinear systems control, various control design methods have been proposed, such as adaptive backstepping control (Zong, Sun et al., 2021), fault-tolerant control (Xu et al., 2014), sliding mode control (Tang et al., 2008) and optimal estimation (Ren et al., 2020, 2022). Among them, adaptive backstepping control has been received a lot of attention because of its advantages in dealing with the uncertainty of the systems (Zhou et al., 2019). However, when the complex nonlinearity occurs in the systems, it is difficult to achieve the desired control effect by using a single control method. Therefore, many methods of combining adaptive control with intelligent control has been proposed, such as adaptive neural networks (NNs) control (Chen et al., 2010; Meng et al., 2015), adaptive fuzzy logic systems (FLSs) control (Li et al., 2011; Tong et al., 2004, 2010) and adaptive multi-dimensional Taylor network (MTN) control (Han, Li et al., 2021; Han et al., 2021; Yan & Duan, 2021; Yan & Kang, 2017). On the other hand, the stochastic disturbances are always inevitable appear in the actual systems and lead to system instability. Therefore, the control research on stochastic nonlinear systems has attracted considerable attention (Ji & Xi, 2006; Wu et al., 2007). Moreover, the above control methods have been successfully applied to stochastic nonlinear systems (Han & Yan, 2018; Hua et al., 2018; Wang et al., 2022). It is noteworthy that as a new kind of approximation method, MTN has been widely studied for their simple structure and good approximation ability, and a large number of research results have been obtained for different systems, such as stochastic nonlinear systems (Han, 2020; Zhu et al., 2022), switched stochastic systems (He et al., 2022) and large-scale stochastic systems (Yan & Han, 2019). However, the

above results only focussed on the controller design and stability analysis of stochastic systems, without taking into account for the full state constraints of the systems. In fact, the full state constraints problem is also an important factor that affects the performance of the systems. Therefore, it is very necessary to solve the full state constraints problem in the research of stochastic nonlinear systems control.

Actually, violating state constraints will reduce the system control performance and even cause the system instability. To solve this problem, many methods have been proposed to realise the full state constraints, such as model predictive control (MPC) (Mayne et al., 2000) and barrier Lyapunov functions (BLFs) methods (Tee et al., 2009). Among them, the BLFs-based method is more widely used because it can realise state constraints without solving the exact solution of the systems. At present, various BLFs have been proposed, such as logarithmic BLFs (Wang, Zong et al., 2021), integral BLFs (Li et al., 2016) and tangent BLFs (Gao et al., 2021). Many interesting results based on BLFs have been reported for various systems, for example, general nonlinear systems (Wang, Zong et al., 2021), stochastic nonlinear systems (Liu et al., 2018), stochastic nonlinear systems with input delay (Li et al., 2022), stochastic nonlinear systems with input saturation (Han, 2022; Li et al., 2021). Nevertheless, there are few research results focus on adaptive fault-tolerant control for stochastic nonlinear systems with full state constraints and multiple faults. In the actual industrial processes, the degradation of system performance or the loss of control of the system caused by multiple faults, including actuator faults and external system faults, is unavoidable. As a hot research topic, it is meaningful to study fault-tolerant control.

In fact, modern industrial systems have the characteristics of high integration and complex structure, which lead to an increase in the probability of system component failure. The failure of different system components might cause the loss of the system performance or stability. Considering the actuator faults in the systems, many effective fault-tolerant control schemes have been designed for different systems, for example, nonlinear systems (Ji et al., 2021; Tong et al., 2014; Wu & Yang, 2016; Yu et al., 2021), switched nonlinear systems (Zhang, Li et al., 2020; Zhang, Shi et al., 2020), stochastic nonlinear systems (Ma et al., 2019; Wang et al., 2019, 2019) and practical systems (Yu et al., 2018; Zong, Yang et al., 2021). It is worth noting that the existence of external faults is also an important factor in destroying the stability of the systems, and some research results have been proposed (Wang et al., 2019). However, research on external faults is still an open issue. For stochastic nonlinear systems with multiple faults, the effectiveness of the above control scheme may be greatly reduced or even ineffective. Therefore, the fault-tolerant control of stochastic nonlinear systems with multiple faults has not been fully studied, which plays an important role in promoting our current research work.

Inspired by the above discussion, for stochastic nonlinear systems with full state constraints, actuator faults and external faults, a new type of adaptive tracking control strategy based on MTN is designed. In this paper, actuator faults composed of lock in place and loss of effectiveness faults are considered. MTN is used to estimate the unknown nonlinearity. BLFs are constructed to avoid violating the full state constraints of the systems. Under the condition of multiple faults, the designed control strategy can still ensure that all signals in the systems remain semi-global ultimately uniformly bounded (SGUUB) in probability, and satisfactory control performance can be obtained. The main innovations of this work are as follows:

- (1) It is the first time that the adaptive fault-tolerant control for a class of stochastic nonlinear systems subject to full state constraints and multiple faults is addressed. As a new type of network, MTN is used to approximate unknown nonlinearities, which only includes addition and multiplication operations. Therefore, the designed adaptive fault-tolerant controller has the advantages of simple structure and low computational complexity.
- (2) Although the issues of full state constraints and actuator faults were studied in Ma et al. (2019) and Wu et al. (2020), the external fault is ignored. Different from the research results in stochastic nonlinear systems (Su & Zhang, 2020; Wang et al., 2019; Wang, Wang et al., 2021), the control scheme proposed in this paper not only overcomes the influence of actuator faults, but also considers the external fault and full state constraints. Especially, in spite of the full state constraints considered in stochastic nonlinear systems (Han, 2022; Li et al., 2022; Liu et al., 2018), the existence of system faults were ignored. Therefore, the above control scheme cannot be directly utilised to dispose of the control problem of the systems considered in this paper.
- (3) It is worth mentioning that there are few studies of multiple faults in the existing results. Although the multiple faults were studied in Wang et al. (2019), only a general

class of nonlinear systems was considered, while stochastic disturbances and full state constraints were not mentioned. Therefore, the systems in Wang et al. (2019) is a special case of the system considered in this paper. In comparison, for a class of stochastic nonlinear systems, full state constraints, actuator faults and external faults are studied in the same framework in this paper. The issues considered are more comprehensive and the results are applicable to more general systems.

2. Problem preparations

2.1 Theoretical preparation

For the convenience of theoretical introduction, considering the following a stochastic nonlinear system

$$d\boldsymbol{\chi} = \boldsymbol{\zeta}(\boldsymbol{\chi}) dt + \boldsymbol{\phi}(\boldsymbol{\chi}) d\omega \quad (1)$$

where $\boldsymbol{\chi} \in \mathfrak{R}^n$ represents the state vector of the system, ω is a r -dimensional standard Wiener process. The local Lipschitz functions $\boldsymbol{\zeta}(\boldsymbol{\chi}) : \mathfrak{R}^n \rightarrow \mathfrak{R}^n$ and $\boldsymbol{\phi}(\boldsymbol{\chi}) : \mathfrak{R}^n \rightarrow \mathfrak{R}^{n \times r}$ satisfy $\boldsymbol{\zeta}(\mathbf{0}) = \mathbf{0}$ and $\boldsymbol{\phi}(\mathbf{0}) = \mathbf{0}$.

Definition 2.1 (Wang et al., 2014): For any function $V(\boldsymbol{\chi}) \in C^2$ associated with the system (1), define the differential operator of $V(\boldsymbol{\chi})$ as follows

$$LV(\boldsymbol{\chi}) = \frac{\partial V(\boldsymbol{\chi})}{\partial \boldsymbol{\chi}} \boldsymbol{\zeta}(\boldsymbol{\chi}) + \frac{1}{2} \text{Tr} \left\{ \boldsymbol{\phi}^T \frac{\partial^2 V(\boldsymbol{\chi})}{\partial \boldsymbol{\chi}^2} \boldsymbol{\phi} \right\} \quad (2)$$

where $\text{Tr}\{\cdot\}$ denotes the trace of \cdot .

Definition 2.2 (Han, 2020): The state $\{\boldsymbol{\chi}(t), t \geq 0\}$ of the system (1) is SGUUB in b th moment, if there are two constants $\varpi > 0$ and $T(\varpi, \boldsymbol{\chi}_0)$, such that $E(|\boldsymbol{\chi}(t)|^b) < \varpi$ for $t > T + t_0$ and any initial state $\boldsymbol{\chi}_0 = \boldsymbol{\chi}(t_0)$.

Lemma 2.1 (Wang et al., 2014): For the Lyapunov function $V(\boldsymbol{\chi}) : \mathfrak{R}^n \rightarrow \mathfrak{R}$ given in Definition 1, there are $\xi_1(\cdot), \xi_2(\cdot) \in \kappa_\infty$ and the positive constants κ_0 and v_0 , if the following inequalities are established

$$\xi_1(|\boldsymbol{\chi}|) \leq V(\boldsymbol{\chi}) \leq \xi_2(|\boldsymbol{\chi}|) \quad (3)$$

$$LV(\boldsymbol{\chi}) \leq -\kappa_0 V(\boldsymbol{\chi}) + v_0 \quad (4)$$

then, the system almost certainly has a unique solution, and the trajectory of the solution is almost bounded, where κ_∞ represents an unbounded set of functions of class κ .

Lemma 2.2 (Hua et al., 2018): (Yang's Inequality) For any real numbers $x \geq 0, y \geq 0$, the following inequality holds

$$xy \leq \frac{\beta^b}{b} |x|^b + \frac{1}{c\beta^c} |y|^c \quad (5)$$

where $\beta > 0, (b-1)(c-1) = 1, b > 1$ and $c > 1$.

2.2 Problem description

In this paper, the following stochastic nonlinear system with unknown control direction is considered

$$\begin{cases} d\chi_i = (h_i(\bar{\chi}_i) \chi_{i+1} + g_i(\bar{\chi}_i)) dt + f_i^T(\bar{\chi}_i) d\omega \\ 1 \leq i \leq n-1 \\ d\chi_n = (\mathbf{h}_n^T \mathbf{u} + g_n(\bar{\chi}_n) + R(t) \Gamma(\chi)) dt + f_n^T(\bar{\chi}_n) d\omega \\ y = \chi_1 \end{cases} \quad (6)$$

where $\mathbf{u} = [u_1, u_2, \dots, u_c]^T \in \mathfrak{R}^c$ is the input vector of the system, u_i is the output of the i th actuator of the system and $y \in \mathfrak{R}$ is the output of the system. $\chi = [\chi_1, \chi_2, \dots, \chi_n]^T \in \mathfrak{R}^n$ represents the state of the system with $\bar{\chi}_i = [\chi_1, \chi_2, \dots, \chi_i]^T \in \mathfrak{R}^i$, all states are restricted to the set $\Xi = \{\chi_i \in \mathfrak{R} \mid |\chi_i| < k_i\}$ with k_i is a positive constant. $h_i(\bar{\chi}_i)$ is an unknown nonlinear function, and \mathbf{h}_n is a known constant vector with $\mathbf{h}_n = [h_{n1}, h_{n2}, \dots, h_{nc}]^T \in \mathfrak{R}^c$. $g_i(\bar{\chi}_i)$ and $f_i(\bar{\chi}_i)$ are nonlinear smooth functions and satisfy $g_i(\mathbf{0}) = \mathbf{0}, f_i(\mathbf{0}) = \mathbf{0}$. In addition, $\Gamma(\chi)$ is the external fault function of the system, and the diagonal matrix $R(t)$ is defined as $R(t) = \begin{cases} 0, & t < T \\ 1, & t \geq T \end{cases}$ with T is the time when an external fault occurs.

Remark 2.1: In the existing results, there are few studies on the control of external faults. Although the multiple faults were studied in Wang et al. (2019), the consideration of external fault was limited to the theoretical level. In fact, the external faults that exist in actual engineered systems are mainly caused by the physical environment or by actual improper operation. For example, the large three-phase induction motors in power systems (Sharma et al., 2015) may have external faults including undervoltage, phase failure, unbalanced voltage, over-voltage and mechanical overload.

For the desired reference signal y_d , the control objectives of this work is to design a suitable controller so that: (a) all signals in the system (6) are SGUUB in probability; (b) the output y tracks the desired reference signal y_d , and the tracking error can be arbitrarily smaller; (c) all states cannot violate their constraint boundaries.

In order to facilitate the further realisation of control objectives, the following preparations are made:

Assumption 2.1 (Gao et al., 2021): *The desired reference signal y_d and its i -th derivative $y_d^{(i)}$ are continuous and bounded for $i = 1, 2, \dots, n$.*

Assumption 2.2 (Su & Zhang, 2020): *For every $i = 1, \dots, n$, the sign of functions $h_i(\bar{\chi}_i)$ and h_{nj} is constant. Furthermore, we assume that $h_i(\bar{\chi}_i) > 0$ and $h_{nj} > 0$, and $h_i(\bar{\chi}_i)$ satisfies*

$$0 < \nu_m \leq h_i(\bar{\chi}_i) \leq \nu_M \quad (7)$$

where $\nu_m > 0$ and $\nu_M > 0$ are constants.

Assumption 2.3 (Liu et al., 2020): *For every $i = 1, 2, \dots, n$, the desired reference signal y_d satisfy $|y_d| \leq \rho_0 \leq k_i$ and $y_d^{(i)} \leq \varpi_i$, where $\rho_0 > 0$ and $\varpi_i > 0$ are constants.*

To achieve the full state constraints, the following Lemma is necessary:

Lemma 2.3 (Liu et al., 2018): *For any positive constant s_a and any $z \in \mathfrak{R}$, if $|z| < s_a$, the following inequality is holds*

$$\log \frac{s_a^{2p}}{s_a^{2p} - z^{2p}} < \frac{z^{2p}}{s_a^{2p} - z^{2p}} \quad (8)$$

where $\log(\cdot)$ is a logarithm of (\cdot) and p is a positive constant.

2.3 Fault description and processing

In this paper, two kinds of actuator faults are considered, including lock in place (LiP) and loss of effective (LoE). According to Su and Zhang (2020), we have

(i) The mathematical expression of LiP:

$$u_i(t) = \underline{u}_i, \quad t \geq t_i, \quad i \in \{i_1, i_2, \dots, i_e\} \subset \{1, 2, \dots, c\} \quad (9)$$

where \underline{u}_i is an unknown constant indicating the location where lock in place fault occurs, and t_i is the moment when it happens.

(ii) The mathematical expression of LoE:

$$u_j(t) = \lambda_j \mu_j, \quad t \geq t_j, \quad j \in \overline{\{i_1, i_2, \dots, i_e\}} \cap \{1, 2, \dots, c\} \quad (10)$$

and $\lambda_j \in [\underline{\lambda}_j, 1], 0 < \underline{\lambda}_j \leq 1$, where μ_j is the applied control input, $\underline{\lambda}_j$ is the lower bound of λ_j and λ_j is the proportion of an actuator that remains effective when losing some of its efficiency. That is to say, if $\lambda_j = 1$, then the i th actuator is without faults. In addition, t_j indicates the moment when the loss of effectiveness fault occurs.

As stated in the work of Su and Zhang (2020), \mathbf{u} can be expressed as follows

$$\mathbf{u}(t) = \lambda \boldsymbol{\mu}(t) + \zeta (\underline{\mathbf{u}} - \lambda \boldsymbol{\mu}(t)) \quad (11)$$

where $\boldsymbol{\mu}(t) = [\mu_1, \mu_2, \dots, \mu_l]^T$ denotes the applied control and $\underline{\mathbf{u}} = [\underline{u}_1, \underline{u}_2, \dots, \underline{u}_l]^T$ with $\underline{u}_i (i = 1, 2, \dots, l)$ is an unknown constant, and there are $\lambda = \text{diag}\{\lambda_1, \lambda_2, \dots, \lambda_l\}$ and $\zeta = \text{diag}\{\zeta_1, \zeta_2, \dots, \zeta_l\}$ with $\zeta_i = \begin{cases} 1, & \text{if } u_i = \underline{u}_i \\ 0, & \text{otherwise} \end{cases}$.

Furthermore, based on the work of Tong et al. (2014) and Su and Zhang (2020), the structure of u_i can be defined as $\mu_i = \sigma_i(\bar{\chi}_n) u_0$, where u_0 is an adaptive controller that needs to be designed later, $0 \leq \underline{\sigma}_i \leq \sigma_i(\bar{\chi}_n) \leq \bar{\sigma}_i, i = 1, 2, \dots, l$, $\underline{\sigma}_i$ and $\bar{\sigma}_i$ are the lower and upper bounds of $\sigma_i(\bar{\chi}_n)$.

2.4 Multi-dimensional Taylor network

The topological structure of MTN is a special NN composed of input layer, intermediate layer and output layer. The related concepts of MTN have been introduced in detail in Yan and Kang (2017), Han et al. (2021), and Han, He et al. (2021), and the following Lemma is introduced.

Lemma 2.4 (Han & Yan, 2018): *Supposing $F(\mathbf{S}) : \mathfrak{R}^n \rightarrow \mathfrak{R}$ is a continuous function defined in compact set Ω , then for any $\varepsilon > 0$, there must exist a MTN expressed as $\boldsymbol{\theta}^T P_{m_n}(\mathbf{S})$ such that*

$$F(\mathbf{S}) = \boldsymbol{\theta}^T P_{m_n}(\mathbf{S}) + \delta(\mathbf{S}) \quad (12)$$

where $\mathbf{S} = [s_1, \dots, s_n]^T \in \mathbb{R}^n$ denotes input layer vector of MTN, $P_{m_n}(\mathbf{S}) = [s_1, \dots, s_n, s_1^2, \dots, s_n^2, \dots, s_1^m, \dots, s_n^m]^T \in \mathbb{R}^l$ is the middle input layer of MTN, $\boldsymbol{\theta} = [\theta_1, \dots, \theta_l]^T \in \mathbb{R}^l$ is weight vector. $\delta(\mathbf{S})$ is the approximation error, which satisfies $|\delta(\mathbf{S})| \leq \varepsilon$.

Remark 2.2: The structure of MTN, as stated in Yan and Kang (2017), Han et al. (2021), and Han, He et al. (2021), is similar to the structure of radial basis function neural network (RBFNN). The difference between the two lies in the way of information processing, namely, the structure of the middle layer is different. Compared with RBFNN, MTN has the following advantages: (i) the computation of the middle layer of MTN contains only addition and multiplication, and the output layer is a linear weighted combination. There is no doubt that the structure of MTN is simpler than RBFNN; (ii) Due to the simple structure of MTN, the complexity of the intermediate layer nonlinear mapping function is reduced, which shortens its training time and improves the convergence speed, and reduces the computational burden.

3. Controller design and stability analysis

3.1 MTN-based control design

In order to design the adaptive control scheme of the system (6), the following coordinate transformation is introduced

$$\begin{cases} z_1 = \chi_1 - y_d \\ z_i = \chi_i - \alpha_{i-1}, \quad i = 2, \dots, n \end{cases} \quad (13)$$

where α_{i-1} is a virtual control signal, which will be designed later.

Step 1: Defining the first BLF as follows

$$V_1 = \frac{1}{4} \log \frac{s_{a1}^4}{s_{a1}^4 - z_1^4} + \frac{1}{2} \boldsymbol{\theta}_1^T \tilde{\boldsymbol{\theta}}_1 \quad (14)$$

where $\tilde{\boldsymbol{\theta}}_1 = \boldsymbol{\theta}_1 - \hat{\boldsymbol{\theta}}_1$ is parameter error, $\hat{\boldsymbol{\theta}}_1$ is the estimated value of $\boldsymbol{\theta}_1$, and $s_{a1} = k_1 - \rho_0$ with ρ_0 is a positive constant.

According to $z_1 = x_1 - y_d$, the derivative of z_1 with respect to time is calculated as follows

$$dz_1 = (h_1 \chi_2 + g_1 - \dot{y}_d) dt + f_1^T d\omega \quad (15)$$

Then, based on Definition 2.1, the following formula is established

$$\begin{aligned} LV_1 &= \Pi_{1,1}^3 (h_1 \chi_2 + g_1 - \dot{y}_d) \\ &+ \frac{1}{2} \Pi_{1,2}^2 (3s_{a1}^4 + z_1^4) \|f_1\|^2 - \tilde{\boldsymbol{\theta}}_1^T \dot{\hat{\boldsymbol{\theta}}}_1 \end{aligned} \quad (16)$$

Remark 3.1: To facilitate the subsequent calculation, $\Pi_{i,\gamma}^\gamma = \frac{z_i^\gamma}{(s_{ai}^4 - z_i^4)^\gamma}$, $i = 1, 2, \dots, n$ is defined, where γ and Υ are constants. For example, in (16), $\Pi_{1,1}^3 = \frac{z_1^3}{s_{a1}^4 - z_1^4}$, $\Pi_{1,2}^2 = \frac{z_1^2}{(s_{a1}^4 - z_1^4)^2}$.

The following inequalities can be obtained by using Young's Inequality

$$\frac{1}{2} \Pi_{1,2}^2 (3s_{a1}^4 + z_1^4) \|f_1\|^2 \leq \frac{\tau_1^2}{4} + \frac{1}{4\tau_1^2} \Pi_{1,4}^4 (3s_{a1}^4 + z_1^4)^2 \|f_1\|^4 \quad (17)$$

$$h_1 z_2 \Pi_{1,1}^3 \leq \frac{1}{4\psi_1^4} h_1 z_2^4 + \frac{3}{4} h_1 \psi_1^{\frac{4}{3}} \Pi_{1,4}^4 \quad (18)$$

where τ_1 and ψ_1 are positive constants.

By substituting (17) and (18) into (16), (16) can be transformed into the following form

$$\begin{aligned} LV_1 &\leq \Pi_{1,1}^3 (h_1 \alpha_1 + N_1) + \frac{1}{4\psi_1^4} h_1 z_2^4 \\ &- \frac{3}{4} \Pi_{1,4}^4 \varphi_1^{\frac{4}{3}} + \frac{\tau_1^2}{4} - \tilde{\boldsymbol{\theta}}_1^T \dot{\hat{\boldsymbol{\theta}}}_1 \end{aligned} \quad (19)$$

where $N_1 = g_1 - \dot{y}_d + \frac{1}{4\tau_1^2} \Pi_{1,3}^3 (3s_{a1}^4 + z_1^4)^2 \|f_1\|^4 + \frac{3}{4} \Pi_{1,1}^3 (h_1 \psi_1^{\frac{4}{3}} + \varphi_1^{\frac{4}{3}})$ and φ_1 is a positive constant.

It is easy to see that item N_1 in (19) is an unknown nonlinear function. From Lemma 2.4, we can approximate it with a MTN, that is

$$N_1 = \boldsymbol{\theta}_1^T P_{m_1}(\mathbf{z}_1) + \delta_1(\mathbf{z}_1) \quad (20)$$

where $\mathbf{z}_1 = [z_1]^T$ is the input vector of MTN, and $|\delta_1(\mathbf{z}_1)| \leq \varepsilon_1$ is the approximation error.

Then, the following inequality is obtained by using Young's Inequality

$$\Pi_{1,1}^3 N_1 \leq \Pi_{1,1}^3 \boldsymbol{\theta}_1^T P_{m_1} + \frac{3}{4} \Pi_{1,4}^4 \varphi_1^{\frac{4}{3}} + \frac{1}{4\varphi_1^4} \varepsilon_1^4 \quad (21)$$

Substituting (21) into (19), and the derivative of V_1 with respect to time is simplified as follows

$$\begin{aligned} LV_1 &\leq \Pi_{1,1}^3 (h_1 \alpha_1 + \boldsymbol{\theta}_1^T P_{m_1}) + \frac{1}{4\psi_1^4} h_1 z_2^4 + \frac{\tau_1^2}{4} \\ &+ \frac{1}{4\varphi_1^4} \varepsilon_1^4 - \tilde{\boldsymbol{\theta}}_1^T \dot{\hat{\boldsymbol{\theta}}}_1 \end{aligned} \quad (22)$$

Then, defining the first virtual control signal as follows

$$\alpha_1 = -\frac{1}{\nu_m} (r_1 z_1 + \hat{\boldsymbol{\theta}}_1^T P_{m_1}) \quad (23)$$

where $\nu_m > 0$ and $r_1 > 0$ are constants.

The term ν_m in (23) is the lower bound of h_1 , that is, $\frac{h_1}{\nu_m} \geq 1$ can be obtained. Then substituting (23) into (22), the following inequality can be easily obtained

$$\begin{aligned} LV_1 &\leq -r_1 \Pi_{1,1}^4 + \frac{1}{4\psi_1^4} h_1 z_2^4 + \frac{\tau_1^2}{4} + \frac{1}{4\varphi_1^4} \varepsilon_1^4 \\ &+ \tilde{\boldsymbol{\theta}}_1^T (\Pi_{1,1}^3 P_{m_1} - \dot{\hat{\boldsymbol{\theta}}}_1) \end{aligned} \quad (24)$$

Step i ($2 \leq i \leq n-1$): Defining the i th BLF as follows

$$V_i = \frac{1}{4} \log \frac{s_{ai}^4}{s_{ai}^4 - z_i^4} + \frac{1}{2} \tilde{\boldsymbol{\theta}}_i^T \tilde{\boldsymbol{\theta}}_i + V_{i-1} \quad (25)$$

where $\tilde{\boldsymbol{\theta}}_i = \boldsymbol{\theta}_i - \hat{\boldsymbol{\theta}}_i$ is parameter error, $\hat{\boldsymbol{\theta}}_i$ is the estimated value of $\boldsymbol{\theta}_i$, $s_{ai} = k_i - \rho_{i-1}$, and ρ_{i-1} is a positive constant.

The time derivative with respect to z_i is as follows

$$dz_i = (h_i \chi_{i+1} + g_i - \nabla \alpha_{i-1}) dt + M_i^T d\omega \tag{26}$$

where for $i = 2, \dots, n$, $\alpha_{i-1} \leq \rho_{i-1}$, $M_i = f_i - \sum_{j=1}^{i-1} \frac{\partial \alpha_{i-1}}{\partial \chi_j} f_j$, and there is $\nabla \alpha_{i-1} = \sum_{j=1}^{i-1} \frac{\partial \alpha_{i-1}}{\partial \chi_j} (h_j \chi_{j+1} + g_j) + \sum_{j=0}^{i-1} \frac{\partial \alpha_{i-1}}{\partial y_d^{(j)}} y_d^{(j+1)} + \sum_{j=1}^{i-1} \frac{\partial \alpha_{i-1}}{\partial \hat{\theta}_j} \dot{\hat{\theta}}_j + \frac{1}{2} \sum_{p,q=1}^{i-1} \frac{\partial^2 \alpha_{i-1}}{\partial \chi_p \partial \chi_q} f_p^T f_q$.

Then, according to (26), LV_i can be calculated as follows

$$LV_i \leq LV_{i-1} + \Pi_{i,1}^3 (h_i \chi_{i+1} + g_i - \nabla \alpha_{i-1}) + \frac{1}{2} \Pi_{i,2}^2 (3s_{ai}^4 + z_i^4) \|M_i\|^2 - \tilde{\theta}_i^T \dot{\hat{\theta}}_i \tag{27}$$

Employing Yang's Inequality, the following inequalities holds

$$\begin{aligned} & \frac{1}{2} \Pi_{i,2}^2 (3s_{ai}^4 + z_i^4)^2 \|M_i\|^2 \\ & \leq \frac{\tau_i^2}{4} + \frac{1}{4\tau_i^2} \Pi_{i,4}^4 (3s_{ai}^4 + z_i^4)^2 \|M_i\|^4 \end{aligned} \tag{28}$$

$$h_i z_{i+1} \Pi_{i,1}^3 \leq \frac{1}{4\psi_i^4} h_i z_{i+1}^4 + \frac{3}{4} h_i \psi_i^{\frac{4}{3}} \Pi_{i,3}^4 \tag{29}$$

where τ_i and ψ_i are positive constants.

According to Mathematical Induction, the following inequality can be obtained

$$LV_{i-1} \leq - \sum_{j=1}^{i-1} \left(r_j \Pi_{j,1}^4 + \frac{\tau_j^2}{4} + \frac{\varphi_j^4 \varepsilon_j^4}{4} + \tilde{\theta}_j^T (\Pi_{j,1}^3 P_{m_j} - \dot{\hat{\theta}}_j) \right) + \frac{1}{4\psi_{i-1}^4} h_{i-1} z_i^4 \tag{30}$$

Substituting (28), (29) and (30) into (27), it is easy to conclude that the following inequality holds

$$LV_i \leq \Pi_{i,1}^3 (h_i \alpha_i + N_i) + \frac{1}{4\psi_i^4} h_i z_{i+1}^4 + \sum_{j=1}^i \frac{\tau_j^2}{4} - \frac{3}{4} \varphi_i^{\frac{4}{3}} \Pi_{i,3}^4 - \tilde{\theta}_i^T \dot{\hat{\theta}}_i + \sum_{j=1}^{i-1} \left(-r_j \Pi_{j,1}^4 + \frac{1}{4} \varphi_j^4 \varepsilon_j^4 + \tilde{\theta}_j^T (\Pi_{j,1}^3 P_{m_j} - \dot{\hat{\theta}}_j) \right) \tag{31}$$

where $N_i = g_i - \nabla \alpha_{i-1} + \frac{h_{i-1} z_i}{4\psi_{i-1}^4 \Pi_{i,1}^3} + \frac{3}{4} \Pi_{i,1}^3 (h_i \psi_i^{\frac{4}{3}} + \varphi_i^{\frac{4}{3}}) + \frac{1}{4\tau_i^2} \Pi_{i,3}^4 (3s_{ai}^4 + z_i^4)^2 \|M_i\|^4$ and φ_i is a positive constant.

It is easy to see that item N_i in (31) is an unknown nonlinear function. From Lemma 2.4, we can approximate it with a MTN, that is

$$N_i = \theta_i^T P_{m_i} (z_i) + \delta_i (z_i) \tag{32}$$

where $z_i = [z_1, z_2, \dots, z_i]^T$ is the input vector of MTN, and $|\delta_i(z_i)| \leq \varepsilon_i$ is the approximation error.

Then, the following inequality is obtained by using Young's Inequality

$$\Pi_{i,1}^3 N_i \leq \Pi_{i,1}^3 \theta_i^T P_{m_i} + \frac{3}{4} \varphi_i^{\frac{4}{3}} \Pi_{i,3}^4 + \frac{\varepsilon_i^4}{4\varphi_i^4} \tag{33}$$

Plugging (33) into (31), and the i th virtual a control signal is designed as follows

$$\alpha_i = -\frac{1}{\upsilon_m} \left(r_i z_i + \hat{\theta}_i^T P_{m_i} \right) \tag{34}$$

where $r_i > 0$ is a constant.

Then, the inequality (31) can be converted into the form as follows

$$LV_i \leq \sum_{j=1}^i \left(-r_j \Pi_{j,1}^4 + \frac{\tau_j^2}{4} + \frac{\varepsilon_j^4}{4\varphi_j^4} + \tilde{\theta}_j^T (\Pi_{j,1}^3 P_{m_j} - \dot{\hat{\theta}}_j) \right) + \frac{1}{4\psi_i^4} h_i z_{i+1}^4 \tag{35}$$

Step n : Defining the n th BLF as follows

$$V_n = \frac{1}{4} \log \frac{s_{an}^4}{s_{an}^4 - z_n^4} + \frac{1}{2} \tilde{\theta}_n^T \tilde{\theta}_n + \frac{1}{2} \tilde{\vartheta}^T \tilde{\vartheta} + V_{n-1} \tag{36}$$

where $\tilde{\theta}_n = \theta_n - \hat{\theta}_n$ and $\tilde{\vartheta} = \vartheta - \hat{\vartheta}$ are parameter errors, $\hat{\theta}_n$ is the estimated value of θ_n , and $\hat{\vartheta}$ is the estimated value of ϑ , $s_{an} = k_n - \rho_{n-1}$ and ρ_{n-1} is a positive constant.

The time derivative with respect to z_n from $z_n = \chi_n - \alpha_{n-1}$ is as follows

$$dz_n = \left(h_n^T B + h_n^T \sum_{j=j_1 \dots j_\eta} u_j + g_n - \nabla \alpha_{n-1} + R\Gamma \right) dt + M_n^T d\omega \tag{37}$$

where $\eta \leq n$ is a positive integer, the set $\{j_1, j_2, \dots, j_\eta\}$ represents the set of actuator indexes with LiP fault, and other indicators, namely $\overline{\{j_1, j_2, \dots, j_\eta\}} \cap \{1, 2, \dots, n\}$, represent that the actuator has an LoE fault. $B = \lambda \mu + \zeta (\underline{u} - \lambda \mu) = \sum_{j \neq j_1 \dots j_\eta} \lambda_j \sigma_j u_0$ and $M_n = f_n - \sum_{j=1}^{n-1} \frac{\partial \alpha_{n-1}}{\partial \chi_j} f_j$.

Then, the derivative of V_n with respect to time can be calculated as follows

$$LV_n = \Pi_{n,1}^3 \left(h_n^T B + h_n^T \sum_{j=j_1 \dots j_\eta} u_j + g_n - \nabla \alpha_{n-1} + R\Gamma \right) - \tilde{\theta}_n^T \dot{\hat{\theta}}_n - \tilde{\vartheta}^T \dot{\hat{\vartheta}} + \frac{1}{2} \Pi_{n,2}^2 (3s_{an}^4 + z_n^4) \|M_n\|^2 + LV_{n-1} \tag{38}$$

Similar to Step i , (38) is further simplified as follows

$$LV_n \leq \Pi_{n,1}^3 \left(u_0 h' + \sum_{j=j_1 \dots j_\eta} h_{nj} u_j + N_n + R\Gamma \right) - \tilde{\theta}_n^T \dot{\hat{\theta}}_n - \tilde{\vartheta}^T \dot{\hat{\vartheta}} - \frac{1}{2} \Pi_{n,2}^6 + \sum_{j=1}^{n-1} \left(-r_j \Pi_{j,1}^4 + \frac{1}{4\varphi_j^4} \varepsilon_j^4 + \tilde{\theta}_j^T (\Pi_{j,1}^3 P_{m_j} - \dot{\hat{\theta}}_j) \right) + \sum_{j=1}^n \frac{\tau_j^2}{4} + \frac{\varepsilon_n^4}{4\varphi_n^4} \tag{39}$$

where $h' = \sum_{j \neq j_1 \dots j_n} h_{nj} \lambda_j \sigma_j$, $N_n = g_n - \nabla \alpha_{n-1} + \frac{3}{4} \varphi_n^{\frac{4}{3}} \Pi_{n,3}^1 + \frac{1}{2} \Pi_{n,1}^3 + \frac{1}{4\tau_n^2} \Pi_{n,3}^1 (3s_{an}^4 + z_n^4)^2 \|M_n\|^4 + \frac{1}{4\psi_{n-1}^4 \Pi_{n,1}^3} h_{n-1} z_n$, τ_n , ψ_n and φ_n are positive constants.

Since N_n is an unknown nonlinear function and cannot be directly used to construct the controller. Therefore, according to Lemma 2.4, N_n can be approximated by a MTN, that is

$$N_n = \theta_n^T P_{m_n}(z_n) + \delta_n(z_n) \tag{40}$$

where $z_n = [z_1, z_2, \dots, z_n]^T$ is the input vector of MTN, and $|\delta_n(z_n)| \leq \varepsilon_n$ is the approximation error.

Similarly, $\Gamma(\chi)$ is also an unknown function and cannot be used directly to build the controller, therefore, for $\forall \varepsilon$, a polynomial $\vartheta^T P_{m_n}(\chi)$ can be found such that

$$\Gamma(\chi) = \vartheta^T P_{m_n}(\chi) + \delta(\chi) \tag{41}$$

where $\chi = [\chi_1, \chi_2, \dots, \chi_n]^T$ is the input vector of MTN, and $\delta(\chi) \leq \varepsilon$ is the approximation error.

Using Young's Inequality, the following inequalities are easily established

$$\Pi_{n,1}^3 N_n \leq \Pi_{n,1}^3 \theta_n^T P_{m_n} + \frac{3}{4} \varphi_n^{\frac{4}{3}} \Pi_{n,3}^4 + \frac{\varepsilon_n^4}{4\varphi_n^4} \tag{42}$$

$$\Pi_{n,1}^3 R\Gamma \leq \Pi_{n,1}^3 \vartheta^T P_{m_n} + \frac{1}{2} \Pi_{n,2}^6 + \frac{1}{2} \varepsilon^2 \tag{43}$$

Substituting (42) and (43) into (39), the following inequality holds

$$\begin{aligned} LV_n \leq & \Pi_{n,1}^3 \left(u_0 h' + \sum_{j=j_1 \dots j_n} h_{nj} u_j + \theta_n^T P_{m_n} + \vartheta^T P_m \right) \\ & - \tilde{\theta}_n^T \dot{\hat{\theta}}_n - \tilde{\vartheta}^T \dot{\hat{\vartheta}} + \frac{1}{2} \varepsilon^2 \\ & + \sum_{j=1}^{n-1} \left(-r_j \Pi_{j,1}^4 + \frac{1}{4\varphi_j^4} \varepsilon_j^4 + \tilde{\theta}_j^T (\Pi_{j,1}^3 P_{m_j} - \dot{\hat{\theta}}_j) \right) \\ & + \sum_{j=1}^n \frac{\tau_j^2}{4} + \frac{\varepsilon_n^4}{4\varphi_n^4} \end{aligned} \tag{44}$$

The n th actual control signal u_0 can be designed by (44) as follows

$$u_0 = -\frac{1}{h'} \left(r_n z_n + \sum_{j=j_1 \dots j_n} h_{nj} u_j + \hat{\theta}_n^T P_{m_n} + \hat{\vartheta}^T P_m + \frac{1}{2} \Pi_{n,1}^3 \right) \tag{45}$$

By substituting u_0 into (44), it is easy to know that the following inequality holds

$$\begin{aligned} LV_n \leq & \sum_{j=1}^n \left(-r_j \Pi_{j,1}^4 + \frac{1}{4\varphi_j^4} \varepsilon_j^4 + \tilde{\theta}_j^T (\Pi_{j,1}^3 P_{m_j} - \dot{\hat{\theta}}_j) + \frac{\tau_j^2}{4} \right) \\ & + \tilde{\vartheta}^T (\Pi_{n,1}^3 P_m - \dot{\hat{\vartheta}}) + \frac{1}{2} \varepsilon^2 \end{aligned} \tag{46}$$

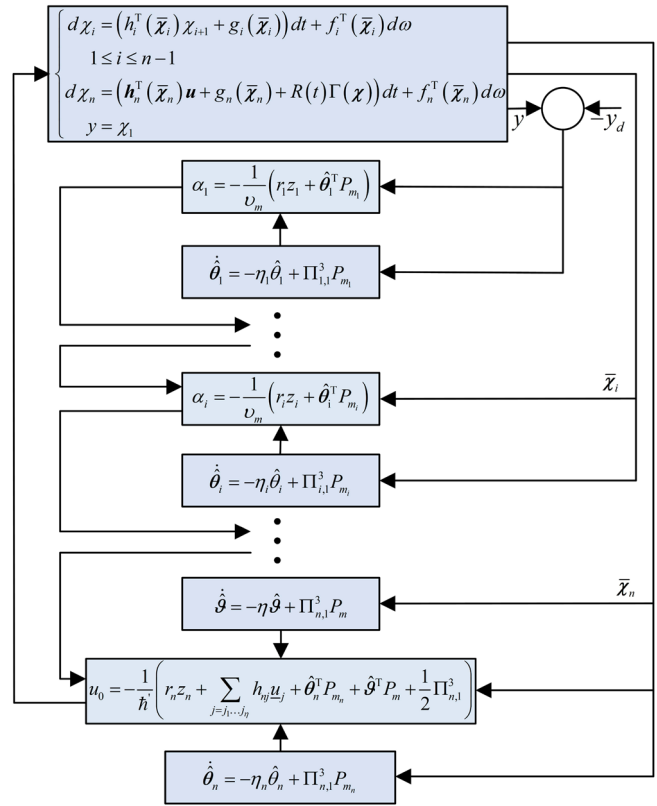


Figure 1. The block diagram of the controlled system.

According to (46), the adaptive laws $\dot{\hat{\theta}}_j$ and $\dot{\hat{\vartheta}}$ are designed as follows

$$\dot{\hat{\theta}}_j = -\eta_j \hat{\theta}_j + \Pi_{j,1}^3 P_{m_j} \tag{47}$$

$$\dot{\hat{\vartheta}} = -\eta \hat{\vartheta} + \Pi_{n,1}^3 P_m \tag{48}$$

where $\eta_j, j = 1, \dots, n$ and η are positive design parameters.

Substituting (47) and (48) into (46), the following inequality is true according to Lemma 2.3

$$\begin{aligned} LV_n \leq & -\sum_{j=1}^n r_j \log \frac{s_{aj}^4}{s_{aj}^4 - z_j^4} + \sum_{j=1}^n \left(\frac{\tau_j^2}{4} + \frac{1}{4\varphi_j^4} \varepsilon_j^4 + \eta_j \tilde{\theta}_j^T \hat{\theta}_j \right) \\ & + \eta \tilde{\vartheta}^T \hat{\vartheta} + \frac{1}{2} \varepsilon^2 \end{aligned} \tag{49}$$

So far, the design process of the control strategy is complete, which is also shown in Figure 1.

Remark 3.2: From the controller design process, we can conclude that the designed adaptive fault-tolerant controller via MTN is significantly decreased in the following two ways: (i) Thanks to the simple structure of MTN, the structure of the controllers (23), (34) and (45) has the advantages of simple structure and small calculations, which only addition and multiplication are involved. (ii) By using the backstepping technique, a recurrent adaptive control strategy based on MTN is proposed, which has traits of clear thinking, and easy operation, so the merits of the proposed approach are that the tuning of the parameter is convenient as well as the design procedure is simple.

3.2 Stability analysis

Theorem 3.1: Under the condition of Assumptions 2.1–2.3, considering the closed-loop system consisting of the controlled nonlinear system (6), the actual controller (45), the virtual control signals (23), (34) and the adaptive laws (47), (48). For any initial condition and there exist positive design parameters $v_m > 0$, η , $r_i > 0$ and η_i , for $i = 1, \dots, n$, then the following properties hold

- (i) The signals in closed-loop system (6) are all SGUUB in probability.
- (ii) The tracking error can converge to a small neighbourhood of the origin.
- (iii) All states of the system never violate the given constraints.

Proof: Selecting the Lyapunov function as follows

$$V = \frac{1}{4} \sum_{i=1}^n \log \frac{s_{ai}^4}{s_{ai}^4 - z_i^4} + \frac{1}{2} \sum_{i=1}^n \tilde{\theta}_i^T \tilde{\theta}_i + \frac{1}{2} \tilde{\vartheta}^T \tilde{\vartheta} \quad (50)$$

According to (49), the derivative of V with respect to time t can be directly calculated as follows

$$LV \leq \sum_{i=1}^n \left(-r_i \log \frac{s_{ai}^4}{s_{ai}^4 - z_i^4} + \frac{\tau_i^2}{4} + \frac{\varepsilon_i^4}{4\varphi_i^4} + \eta_i \tilde{\theta}_i^T \hat{\theta}_i \right) + \eta \tilde{\vartheta}^T \hat{\vartheta} + \frac{1}{2} \varepsilon^2 \quad (51)$$

According to Young's Inequality, the items $\eta_i \tilde{\theta}_i^T \hat{\theta}_i$ and $\eta \tilde{\vartheta}^T \hat{\vartheta}$ in (51) can be transformed into the following inequalities

$$\eta_i \tilde{\theta}_i^T \hat{\theta}_i \leq -\frac{1}{2} \eta_i \tilde{\theta}_i^T \tilde{\theta}_i + \frac{1}{2} \eta_i \theta_i^T \theta_i \quad (52)$$

$$\eta \tilde{\vartheta}^T \hat{\vartheta} \leq -\frac{1}{2} \eta \tilde{\vartheta}^T \tilde{\vartheta} + \frac{1}{2} \eta \vartheta^T \vartheta \quad (53)$$

By substituting (52) and (53) into (51), the following inequality can be established

$$LV \leq -\sum_{i=1}^n \left(r_i \log \frac{s_{ai}^4}{s_{ai}^4 - z_i^4} + \frac{1}{2} \eta_i \tilde{\theta}_i^T \tilde{\theta}_i \right) - \frac{1}{2} \eta \tilde{\vartheta}^T \tilde{\vartheta} + \sum_{i=1}^n \left(\frac{\tau_i^2}{4} + \frac{1}{4\varphi_i^4} \varepsilon_i^4 + \frac{1}{2} \eta_i \theta_i^T \theta_i \right) + \frac{1}{2} \eta \vartheta^T \vartheta + \frac{1}{2} \varepsilon^2 \quad (54)$$

Then, denoting κ_0 and v_0 are defined as $\kappa_0 = \min\{4r_i, 2\eta_i, 2\eta : i = 1, 2, \dots, n\}$ and $v_0 = \sum_{i=1}^n \left(\frac{\tau_i^2}{4} + \frac{1}{4\varphi_i^4} \varepsilon_i^4 + \frac{1}{2} \eta_i \theta_i^T \theta_i \right) + \frac{1}{2} \eta \vartheta^T \vartheta + \frac{1}{2} \varepsilon^2$, (54) can be rewritten as follows

$$LV \leq -\kappa_0 V + v_0 \quad (55)$$

Based on Lemma 2.1, (55) further implies that

$$0 \leq E[V(t)] \leq V(0) e^{-\kappa_0 t} + \frac{v_0}{\kappa_0} \quad (56)$$

Based on the above work, it is easy to conclude that the bound of $E[V(0)]$ is $\frac{v_0}{\kappa_0}$, which also shows that all signals of the closed-loop system (6) are SGUUB in probability.

According to Assumption 2.3 and the definitions are given in the backstepping process, there are $\chi_1 = z_1 + y_d$ and $|y_d| \leq \rho_0$, it can be seen from this that $|\chi_1| \leq |z_1| + |y_d| \leq s_{a1} + \rho_0$. Define $s_{a1} = k_1 - \rho_0$, then it has $|\chi_1| \leq k_1$. Since $\chi_i = z_i + \alpha_{i-1}$ and $\alpha_{i-1} \leq \rho_{i-1}$, one has that $|\chi_i| \leq |z_i| + |\alpha_{i-1}| = s_{ai} + \rho_{i-1}$. Based on $s_{ai} = k_i - \rho_{i-1}$, $|\chi_i| \leq k_i$ can be easily obtained. That is to say, all the states in the closed-loop system are constrained within the given constraints.

Further, $|z_i| \leq s_{ai} \sqrt[4]{1 - e^{-4V(0) - 4\frac{v_0}{\kappa_0}}}$ can be obtained, this shows that the tracking error z_1 is bounded and can be arbitrarily reduced by selecting appropriate design parameters. ■

4. Simulation experiment

In this section, three examples are presented to verify the effectiveness and applicability of the proposed control strategy.

Example 4.1: The following second-order stochastic nonlinear system with multiple faults and full-state constraints are considered

$$\begin{cases} d\chi_1 = (\chi_2 + 0.1\chi_1) dt + 0.1\chi_1 d\omega \\ d\chi_2 = (0.8u_1 + 0.8u_2 + 0.8\chi_1\chi_2 \\ \quad + 8R\chi_2 \sin \chi_1) dt + 0.2\chi_2^2 d\omega \\ y = \chi_1 \end{cases} \quad (57)$$

The initial condition is given as $\chi_1(0) = \chi_2(0) = 0$, the states χ_1 and χ_2 are restricted to $|\chi_1| \leq 1$ and $|\chi_2| \leq 1$, respectively. The desired reference signal is selected as $y_d = 0.5(\sin t + \sin(0.5t))$.

According to Theorem 3.1, the virtual control signals, the actual control input and the adaptive laws are selected as (23), (34), (45), (47) and (48), respectively. The external fault occurs at $t = 15s$, and the actuator faults are expressed by $u_1 = \underline{u}_1 = 1$ and $u_2 = 0.8u_0$ for $t \geq 10s$. In simulation, the design parameters are selected as follows: $\eta = 0.5$, $\eta_1 = 1$, $\eta_2 = 1$, $r_1 = 3$, $r_2 = 10$, $v_m = 0.1$, $h_{21} = h_{22} = 0.8$, $\lambda_1 = \lambda_2 = 0.8$ and $\sigma_1 = \sigma_2 = 1$. The simulation results are shown in Figures 2–5.

As can be seen from Figure 2, the system output y tracks the desired reference signal y_d , and a satisfactory tracking effect is obtained. It can be clearly seen from Figure 3 that the tracking error is constrained in a small neighbourhood of the origin. Figures 2 and 4 illustrate that the states χ_1 and χ_2 are constrained within a given boundary range. The trajectory of the control input u in Figure 3 and the fault function Γ in Figure 5 indicate that the actuator faults occur at $t = 10$ and the external fault occurs at $t = 15$. According to the simulation results, we can draw the conclusion that all signals in the system can maintain SGUUB in probability after the faults of the system, and the tracking effect is still satisfactory. Therefore, Figures 2–5 verifies the effectiveness of the proposed control strategy.

Example 4.2: To further illustrate the applicability of the proposed scheme, a single link manipulator subject to external disturbances and multiple faults are considered. Similarly to Wang

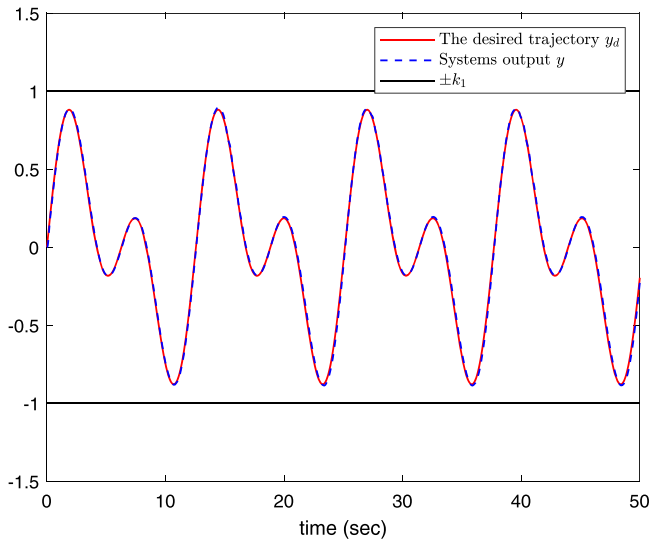


Figure 2. The trajectories of the output y and the desired signal y_d .

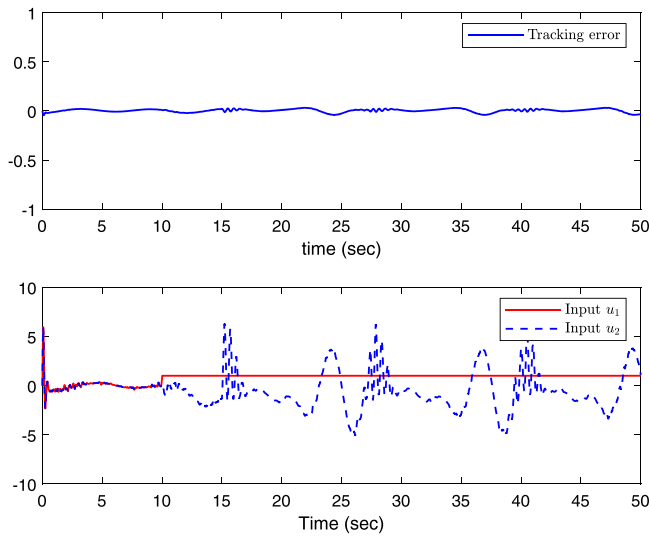


Figure 3. The trajectories of the tracking error and control inputs u_1, u_2 .

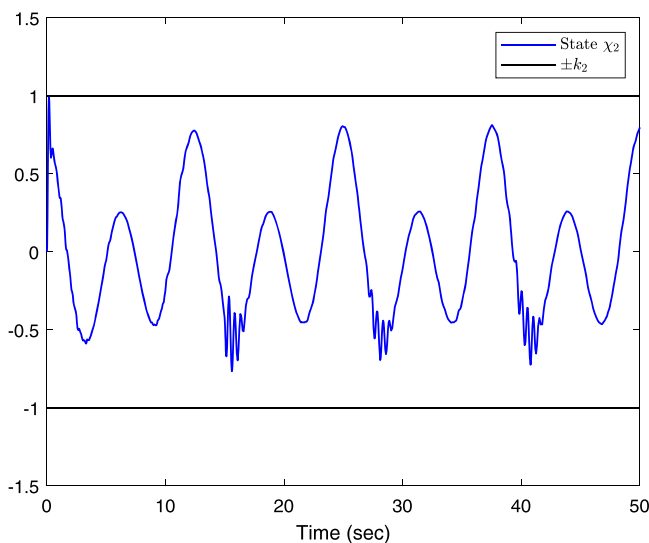


Figure 4. The trajectory of system state χ_2 .

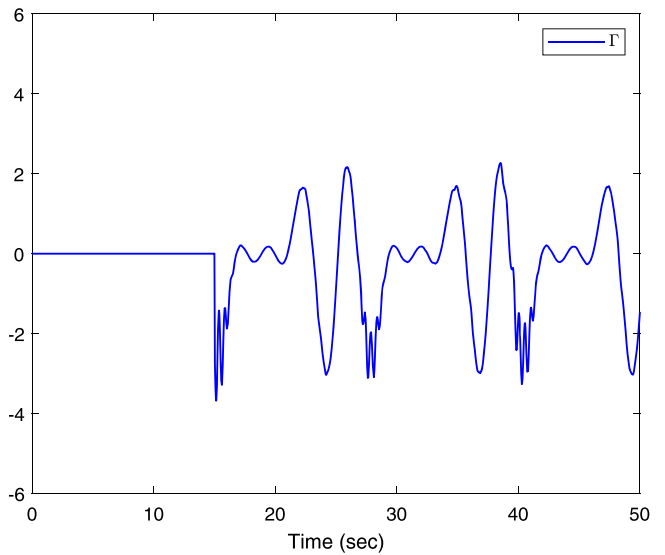


Figure 5. The trajectory of external fault.

et al. (2020), its dynamic system can be expressed as follows

$$\begin{cases} D\ddot{q} + E\dot{q} + H \sin(q) = v + v_d \\ M\dot{v} + Qv = \mathbf{b}^T u - K_m \dot{q} \end{cases} \quad (58)$$

where q, \dot{q}, \ddot{q} denote the angular position, the velocity, and the acceleration of the link, respectively. u represents control input, \mathbf{b} denotes the vector of unknown constants, v and $v_d = q^2 \cos(\dot{q}v)$ denote torque and the external disturbances, respectively. The parameters of system (58), including D, E, H, M, Q and K_m , are the same as Wang et al. (2020).

Define $\chi_1 = q, \chi_2 = \dot{q}, \chi_3 = \tau$, and let $\mathbf{b} = [10, 10]^T$, the system (58) can be rewritten as

$$\begin{cases} d\chi_1 = \chi_2 dt \\ d\chi_2 = (\chi_3 + \chi_1^2 \cos(\chi_2 \chi_3) - 10 \sin(\chi_1) - \chi_2) dt + \chi_2 d\omega \\ d\chi_3 = (10u_1 + 10u_2 - 2\chi_2 - 10\chi_3 \\ \quad + R\chi_3 \sin(\chi_1 \chi_2 \chi_3)) dt + 0.1\chi_3 d\omega \\ y = \chi_1 \end{cases} \quad (59)$$

with the initial condition is given as $\chi_1(0) = \chi_2(0) = \chi_3(0) = 0$ and the desired reference signal is selected as $y_d = 0.5(\sin t + \sin(0.5t))$.

In simulation, the external fault occurs at $t = 15s$, and the actuator faults are expressed by $u_1 = \underline{u}_1 = 5$ and $u_2 = 0.8u_0$ for $t \geq 10s$. The states χ_1, χ_2 and χ_3 are restricted to $|\chi_1| \leq 1, |\chi_2| \leq 1.5$ and $|\chi_3| \leq 8$, respectively. The design parameters are selected as follows: $\eta = 3, \eta_1 = 0.1, \eta_2 = 3, \eta_3 = 0.1, r_1 = 10, r_2 = 13, r_3 = 5, v_m = 1, h_{31} = h_{32} = 10, \lambda_1 = \lambda_2 = 0.8$ and $\sigma_1 = \sigma_2 = 2$. The simulation results are shown in Figures 6–9.

As shown in Figures 6 and 7, a good tracking performance is obtained, namely, the system output y can follow the desired reference signal y_d well. It is obvious from Figures 6–9 that all states in the closed-loop system are constrained within the given constraint limits, and all states can still be maintained SGUUB

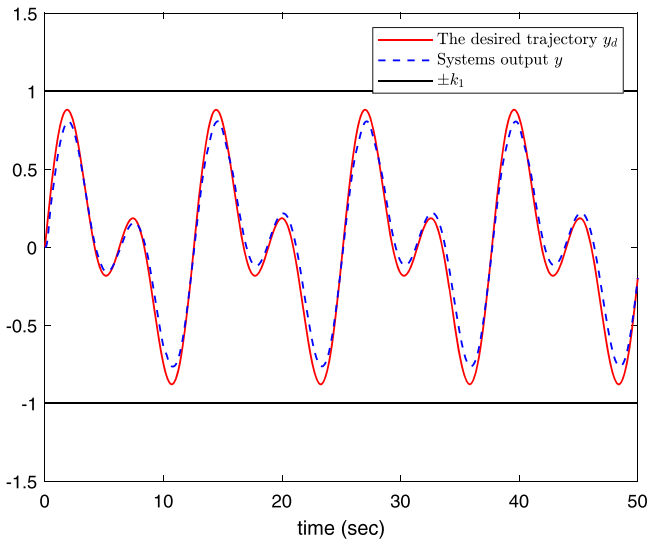


Figure 6. The trajectories of the output y and the desired signal y_d .

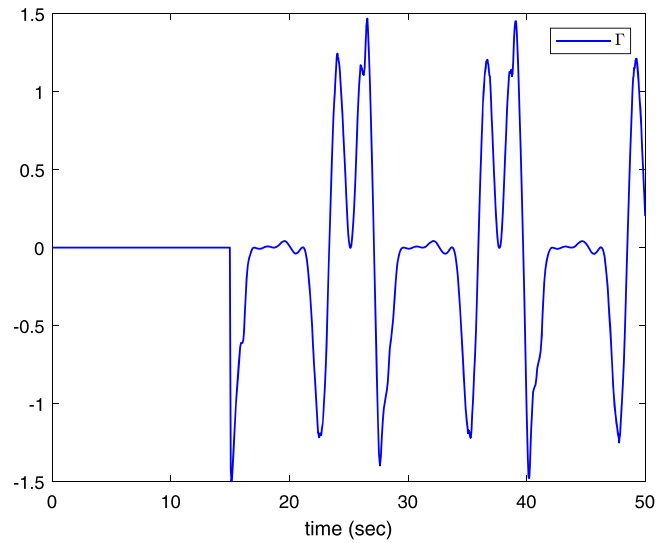


Figure 9. The trajectory of external fault curve.

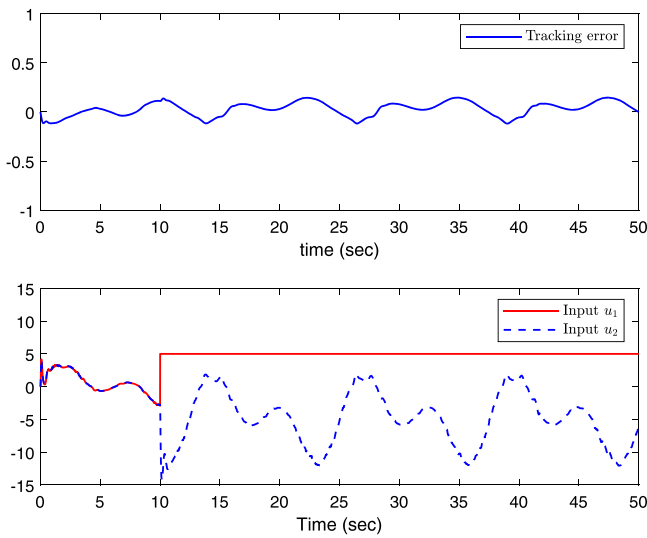


Figure 7. The trajectories of the tracking error and control inputs u_1, u_2 .

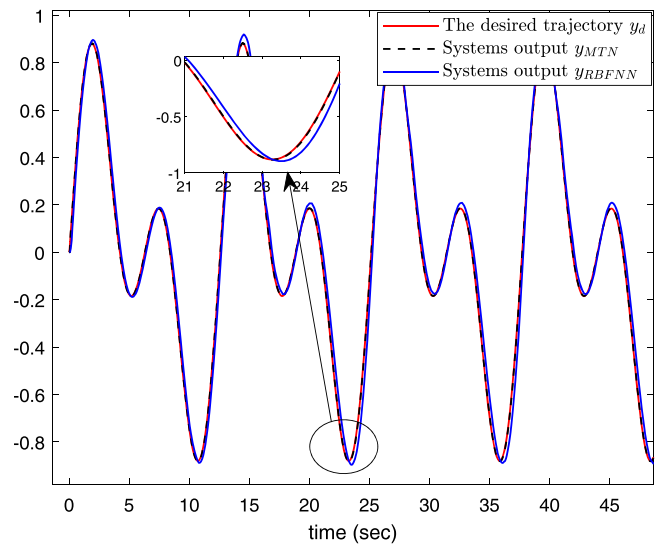


Figure 10. Trajectory comparison results of MTN and RBFNN.

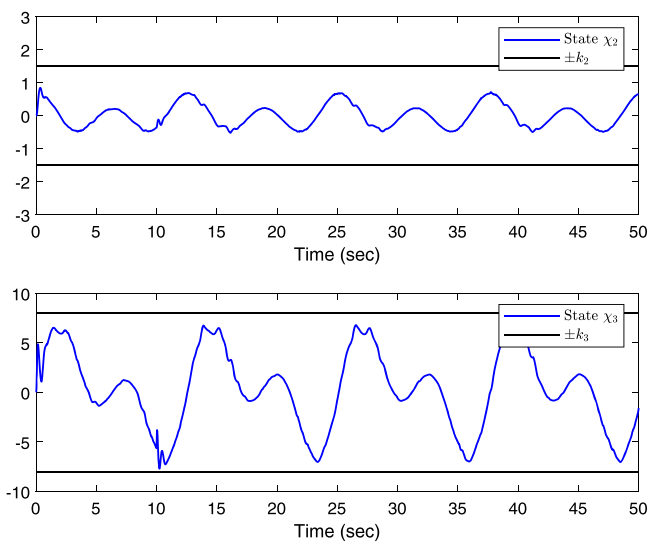


Figure 8. The trajectories of system state χ_2 and χ_3 .

in probability after multiple faults of the system. The excellent simulation results of Example 2 show that the proposed control strategy is practical. To sum up, the control strategy proposed in this paper is feasible and effective.

Remark 4.1: In Examples 4.1 and 4.2, a combination of sine signals oscillating at the origin is selected as the desired reference signal, which is a common reference signal that can be found in the tracking control problem of nonlinear systems (Han, 2020, 2022; Ji & Xi, 2006; Su & Zhang, 2020; Wang et al., 2019, 2014). It is noteworthy that the signal $y_d = 0.5(\sin t + \sin(0.5t))$ is selected as the desired reference signal for simulation experiments, however, it can be displaced by other signals satisfy Assumption 2.1.

Example 4.3: For the stochastic nonlinear system (57) in Example 1, RBFNNs are employed to replace MTNs in the control structure, including the actual control input, the virtual

control signals and the adaptive laws. The tracking effect under two kinds of approximators are shown in Figure 10.

From Figure 10, it can be seen that effective tracking can be achieved by using the above two methods. However, it is worth noting that the MTN-based control method has a better tracking effect, which can be seen from the local subgraph. Therefore, we can conclude that when the tracking control is implemented, MTN-based control approach can get a relatively better tracking performance with low computational.

5. Conclusion

In this work, the adaptive control problem for a class of stochastic nonlinear systems with multiple faults and full state constraints is studied, and an adaptive fault-tolerant control strategy based on MTN is proposed. BLFs are constructed to implement full-state constraints. MTN is used to approximate the unknown nonlinearity in the system, and an adaptive fault-tolerant controller is constructed by combining MTN with backstepping technology. The designed controller has the characteristics of a simple structure and low calculation complexity. Three simulation examples show that the proposed control strategy can not only ensure good tracking performance, but also avoid all states in the closed-loop system from violating the given range. Simulation results verify the effectiveness and practicability of the proposed control strategy.

Disclosure statement

No potential conflict of interest was reported by the author(s).

Funding

This work was supported by the Shandong Provincial Natural Science Foundation, China [grant number ZR2020QF055].

ORCID

Na Li  <http://orcid.org/0000-0002-7911-8903>

Yu-Qun Han  <http://orcid.org/0000-0001-9847-9627>

Wen-Jing He  <http://orcid.org/0000-0001-6370-592X>

Shan-Liang Zhu  <http://orcid.org/0000-0002-6194-3614>

References

- Chen, M., Ge, S. S., & How, B. V. E. (2010). Robust adaptive neural network control for a class of uncertain MIMO nonlinear systems with input nonlinearities. *IEEE Transactions on Neural Networks*, 21(5), 796–812. <https://doi.org/10.1109/TNN.2010.2042611>
- Gao, T. T., Liu, Y. J., Li, D. P., Tong, S. C., & Li, T. S. (2021). Adaptive neural control using tangent time-varying BLFs for a class of uncertain stochastic nonlinear systems with full state constraints. *IEEE Transactions on Cybernetics*, 51(4), 1943–1953. <https://doi.org/10.1109/TCYB.2021.20136>
- Han, Y. Q. (2020). Adaptive tracking control for a class of stochastic non-linear systems with input delay: A novel approach based on multi-dimensional Taylor network. *IET Control Theory and Applications*, 14(15), 2147–2153. <https://doi.org/10.1049/cth2.v14.15>
- Han, Y. Q. (2022). Adaptive control of a class of stochastic nonlinear systems with full state constraints and input saturation using multi-dimensional Taylor network. *Asian Journal of Control*, 24(4), 1609–1621. <https://doi.org/10.1002/asjc.v24.4>
- Han, Y. Q., He, W. J., Li, N., & Zhu, S. L. (2021). Adaptive tracking control of a class of nonlinear systems with input delay and dynamic uncertainties using multi-dimensional Taylor network. *International Journal of Control, Automation and Systems*, 19(12), 4078–4089. <https://doi.org/10.1007/s12555-020-0708-y>
- Han, Y. Q., Li, N., He, W. J., & Zhu, S. L. (2021). Adaptive multi-dimensional Taylor network funnel control of a class of nonlinear systems with asymmetric input saturation. *International Journal of Adaptive Control and Signal Processing*, 35(5), 713–726. <https://doi.org/10.1002/acs.v35.5>
- Han, Y. Q., & Yan, H. S. (2018). Adaptive multi-dimensional Taylor network tracking control for SISO uncertain stochastic non-linear systems. *IET Control Theory and Applications*, 12(8), 1107–1115. <https://doi.org/10.1049/cth2.v12.8>
- Han, Y. Q., Zhu, S. L., Yang, S. G., & Chu, L. (2021). Adaptive multi-dimensional Taylor network tracking control for a class of nonlinear systems. *International Journal of Control*, 94(2), 277–285. <https://doi.org/10.1080/00207179.2019.1590649>
- He, W. J., Zhu, S. L., Li, N., & Han, Y. Q. (2022). Adaptive controller design for switched stochastic nonlinear systems subject to unknown dead-zone input via new type of network approach. *International Journal of Control Automation and Systems*, (Accepted).
- Hua, C. C., Li, K., & Guan, X. P. (2018). Event-based dynamic output feedback adaptive fuzzy control for stochastic nonlinear systems. *IEEE Transactions on Fuzzy Systems*, 26(5), 3004–3015. <https://doi.org/10.1109/TFUZZ.91>
- Ji, H. B., & Xi, H. S. (2006). Adaptive output-feedback tracking of stochastic nonlinear systems. *IEEE Transactions on Automatic Control*, 51(2), 355–360. <https://doi.org/10.1109/TAC.2005.863501>
- Ji, R. H., Ma, J., Li, D. Y., & Ge, S. S. (2021). Finite-time adaptive output feedback control for MIMO nonlinear systems with actuator faults and saturations. *IEEE Transactions on Fuzzy Systems*, 29(8), 2256–2270. <https://doi.org/10.1109/TFUZZ.2020.2996709>
- Li, C. Y., Tong, S. C., & Wang, W. (2011). Fuzzy adaptive high-gain-based observer backstepping control for SISO nonlinear systems. *Information Sciences*, 181(11), 2405–2421. <https://doi.org/10.1016/j.ins.2011.01.040>
- Li, D. J., Li, J., & Li, S. (2016). Adaptive control of nonlinear systems with full state constraints using integral barrier Lyapunov functionals. *Neurocomputing*, 186, 90–96. <https://doi.org/10.1016/j.neucom.2015.12.075>
- Li, N., Han, Y. Q., He, W. J., & Zhu, S. L. (2022). Control design for stochastic nonlinear systems with full-state constraints and input delay: A new adaptive approximation method. *International Journal of Control, Automation and Systems*, 20(8), 2768–2778. <https://doi.org/10.1007/s12555-021-0451-z>
- Li, Y. L., Niu, B., Zong, G. D., Zhao, J. F., & Zhao, X. D. (2021). Command filter-based adaptive neural finite-time control for stochastic nonlinear systems with time-varying full-state constraints and asymmetric input saturation. *International Journal of Systems Science*, 52(1), 199–221. <https://doi.org/10.1080/00207721.2021.1943562>
- Liu, L., Gao, T. T., Liu, Y. J., & Tong, S. C. (2020). Time-varying asymmetrical BLFs based adaptive finite-time neural control of nonlinear systems with full state constraints. *IEEE/CAA Journal of Automatica Sinica*, 7(5), 1335–1343. <https://doi.org/10.1109/JAS.2020.1003213>
- Liu, Y. J., Lu, S. M., Tong, S. C., Chen, X. K., Chen, C. L. P., & Li, D. J. (2018). Adaptive control-based barrier Lyapunov functions for a class of stochastic nonlinear systems with full state constraints. *Automatica*, 87, 83–93. <https://doi.org/10.1016/j.automatica.2017.07.028>
- Ma, H., Li, H. Y., Liang, H. J., & Dong, G. W. (2019). Adaptive fuzzy event-triggered control for stochastic nonlinear systems with full state constraints and actuator faults. *IEEE Transactions on Fuzzy Systems*, 27(11), 2242–2254. <https://doi.org/10.1109/TFUZZ.91>
- Mayne, D. Q., Rawlings, J. B., Rao, C. V., & Scokaert, P. O. M. (2000). Constrained model predictive control: Stability and optimality. *Automatica*, 36(6), 789–814. [https://doi.org/10.1016/S0005-1098\(99\)00214-9](https://doi.org/10.1016/S0005-1098(99)00214-9)
- Meng, W. C., Yang, Q. M., & Sun, Y. X. (2015). Adaptive neural control of nonlinear MIMO systems with time-varying output constraints. *IEEE Transactions on Neural Networks and Learning Systems*, 26(5), 1074–1085. <https://doi.org/10.1109/TNNLS.2014.2333878>
- Ren, H. R., Lu, R. Q., Xiong, J. L., & Xu, Y. (2020). Optimal estimation for discrete-time linear system with communication constraints and measurement quantization. *IEEE Transactions on Systems, Man, and Cybernetics: System*, 50(5), 1932–1942. <https://doi.org/10.1109/TSMC.2018.2792009>

- Ren, H. R., Wang, Y., Liu, M., & Li, H. Y. (2022). An optimal estimation framework of multi-agent systems with random transport protocol. *IEEE Transactions on Signal Processing*, 70, 2548–2559. <https://doi.org/10.1109/TSP.2022.3175020>
- Sharma, S., Malik, H., & Khatri, A. (2015). External fault classification experienced by three-phase induction motor based on multi-class ELM. *Procedia Computer Science*, 70, 814–820. <https://doi.org/10.1016/j.procs.2015.10.122>
- Su, H., & Zhang, W. H. (2020). Adaptive fuzzy tracking control for a class of nonstrict-feedback stochastic nonlinear systems with actuator faults. *IEEE Transactions on Systems, Man, and Cybernetics: Systems*, 50(9), 3456–3469. <https://doi.org/10.1109/TSMC.2020.1021021>
- Tang, G. Y., Dong, R., & Gao, H. W. (2008). Optimal sliding mode control for nonlinear systems with time-delay. *Nonlinear Analysis: Hybrid Systems*, 2(3), 891–899. <https://doi.org/10.1016/j.nahs.2008.02.003>
- Tee, K. P., Ge, S. S., & Tay, E. H. (2009). Barrier Lyapunov functions for the control of output-constrained nonlinear systems. *Automatica*, 45(4), 918–927. <https://doi.org/10.1016/j.automatica.2008.11.017>
- Tong, S. C., Huo, B. Y., & Li, Y. M. (2014). Observer-based adaptive decentralized fuzzy fault-tolerant control of nonlinear large-scale systems with actuator failures. *IEEE Transactions on Fuzzy Systems*, 22(1), 1–15. <https://doi.org/10.1109/TFUZZ.2013.2241770>
- Tong, S. C., Li, H. X., & Wang, W. (2004). Observer-based adaptive fuzzy control for SISO nonlinear systems. *Fuzzy Sets and Systems*, 148(3), 355–376. <https://doi.org/10.1016/j.fss.2003.11.017>
- Tong, S. C., Liu, C. L., & Li, Y. M. (2010). Fuzzy-adaptive decentralized output-feedback control for large-scale nonlinear systems with dynamical uncertainties. *IEEE Transactions on Fuzzy Systems*, 18(5), 845–861. <https://doi.org/10.1109/TFUZZ.2010.2050326>
- Wang, F., Liu, Z., Zhang, Y., & Chen, C. L. P. (2019). Adaptive finite-time control of stochastic nonlinear systems with actuator failures. *Fuzzy Sets and Systems*, 374, 170–183. <https://doi.org/10.1016/j.fss.2018.12.005>
- Wang, F., You, Z. Y., Liu, Z., & Chen, C. L. P. (2022). A fast finite-time neural network control of stochastic nonlinear systems. *IEEE Transactions on Neural Networks and Learning Systems*, 1–10. <https://doi.org/10.1109/TNNLS.2022.3143655>
- Wang, H. Q., Bai, W., & Liu, P. X. (2019). Finite-time adaptive fault-tolerant control for nonlinear systems with multiple faults. *IEEE/CAA Journal of Automatica Sinica*, 6(6), 1417–1427. <https://doi.org/10.1109/JAS.6570654>
- Wang, H. Q., Chen, B., Liu, K. F., Liu, X. P., & Lin, C. (2014). Adaptive neural tracking control for a class of nonstrict-feedback stochastic nonlinear systems with unknown backlash-like hysteresis. *IEEE Transactions on Neural Networks and Learning Systems*, 25(5), 947–958. <https://doi.org/10.1109/TNNLS.2013.2283879>
- Wang, H. Q., Liu, P. X., Zhao, X. D., & Liu, X. P. (2020). Adaptive fuzzy finite-time control of nonlinear systems with actuator faults. *IEEE Transactions on Cybernetics*, 50(5), 1786–1797. <https://doi.org/10.1109/TCYB.6221036>
- Wang, J. H., Liu, Z., Chen, C. L. P., & Zhang, Y. (2019). Fuzzy adaptive compensation control of uncertain stochastic nonlinear systems with actuator failures and input hysteresis. *IEEE Transactions on Cybernetics*, 49(1), 2–13. <https://doi.org/10.1109/TCYB.2017.2758025>
- Wang, L. B., Wang, H. Q., & Liu, P. X. (2021). Adaptive fuzzy finite-time control of stochastic nonlinear systems with actuator faults. *Nonlinear Dynamics*, 104(1), 523–536. <https://doi.org/10.1007/s11071-021-06309-2>
- Wang, Y. D., Zong, G. D., Yang, D., & Shi, K. B. (2021). Finite-time adaptive tracking control for a class of nonstrict feedback nonlinear systems with full state constraints. *International Journal of Robust and Nonlinear Control*, 32(5), 2551–2569. <https://doi.org/10.1002/rnc.v32.5>
- Wu, L. B., Park, J. H., & Zhao, N. N. (2020). Robust adaptive fault-tolerant tracking control for nonaffine stochastic nonlinear systems with full-state constraints. *IEEE Transactions on Cybernetics*, 50(8), 3793–3805. <https://doi.org/10.1109/TCYB.6221036>
- Wu, L. B., & Yang, G. H. (2016). Robust adaptive fault-tolerant control for a class of uncertain nonlinear systems with multiple time delays. *Journal of Process Control*, 41, 1–13. <https://doi.org/10.1016/j.jprocont.2016.02.001>
- Wu, Z. J., Xie, X. J., & Zhang, S. Y. (2007). Adaptive backstepping controller design using stochastic small-gain theorem. *Automatica*, 43(4), 608–620. <https://doi.org/10.1016/j.automatica.2006.10.020>
- Xu, Y. Y., Tong, S. C., & Li, Y. M. (2014). Prescribed performance fuzzy adaptive fault-tolerant control of non-linear systems with actuator faults. *IET Control Theory & Applications*, 8(6), 420–431. <https://doi.org/10.1049/cth2.v8.6>
- Yan, H. S., & Duan, Z. Y. (2021). Tube-based model predictive control using multidimensional Taylor network for nonlinear time-delay systems. *IEEE Transactions on Automatic Control*, 66(5), 2099–2114. <https://doi.org/10.1109/TAC.2020.3005674>
- Yan, H. S., & Han, Y. Q. (2019). Decentralized adaptive multi-dimensional Taylor network tracking control for a class of large-scale stochastic nonlinear systems. *International Journal of Adaptive Control and Signal Processing*, 33(4), 664–683. <https://doi.org/10.1002/acs.v33.4>
- Yan, H. S., & Kang, A. M. (2017). Asymptotic tracking and dynamic regulation of SISO non-linear system based on discrete multi-dimensional Taylor network. *IET Control Theory and Applications*, 11(10), 1619–1626. <https://doi.org/10.1049/cth2.v11.10>
- Yu, X., Li, P., & Zhang, Y. M. (2018). The design of fixed-time observer and finite-time fault-tolerant control for hypersonic gliding vehicles. *IEEE Transactions on Industrial Electronics*, 65(5), 4135–4144. <https://doi.org/10.1109/TIE.41>
- Yu, X. H., Wang, T., Qiu, J. B., & Gao, H. J. (2021). Barrier Lyapunov function-based adaptive fault-tolerant control for a class of strict-feedback stochastic nonlinear systems. *IEEE Transactions on Cybernetics*, 51(2), 938–946. <https://doi.org/10.1109/TCYB.6221036>
- Zhang, J., Li, S., & Xiang, Z. R. (2020). Adaptive fuzzy finite-time fault-tolerant control for switched nonlinear large-scale systems with actuator and sensor faults. *Journal of the Franklin Institute*, 357(16), 11629–11644. <https://doi.org/10.1016/j.jfranklin.2019.09.005>
- Zhang, M., Shi, P., Shen, C., & Wu, Z. G. (2020). Static output feedback control of switched nonlinear systems with actuator faults. *IEEE Transactions on Fuzzy Systems*, 28(8), 1600–1609. <https://doi.org/10.1109/TFUZZ.91>
- Zhou, J., Wen, C. Y., Wang, W., & Yang, F. (2019). Adaptive backstepping control of nonlinear uncertain systems with quantized states. *IEEE Transactions on Automatic Control*, 64(11), 4756–4763. <https://doi.org/10.1109/TAC.9>
- Zhu, S. L., Wang, M. X., & Han, Y. Q. (2022). Adaptive finite-time control for stochastic nonlinear systems using multi-dimensional Taylor network. *Transactions of the Institute of Measurement and Control*, 44(2), 457–467. <https://doi.org/10.1177/01423312211039629>
- Zong, G. D., Sun, H. B., & Nguang, S. K. (2021). Decentralized adaptive neuro-output feedback saturated control for INS and its application to AUV. *IEEE Transactions on Neural Networks and Learning Systems*, 32(12), 5492–5501. <https://doi.org/10.1109/TNNLS.2021.3050992>
- Zong, G. D., Yang, D., Lam, J., & Song, X. Q. (2021). Fault-tolerant control of switched LPV systems: A bumpless transfer approach. *IEEE/ASME Transactions on Mechatronics*, 27(3), 1436–1446. <https://doi.org/10.1109/TMECH.2021.3096375>